Functional Ecology

British Ecological Society

Functional Ecology 2015, **29**, 1587–1602 doi: 10.1111/1365-2435.12470

Size-related scaling of tree form and function in a mixed-age forest

Kristina J. Anderson-Teixeira*[,1,2], Jennifer C. McGarvey[2], Helene C. Muller-Landau[1], Janice Y. Park[2], Erika B. Gonzalez-Akre[2], Valentine Herrmann[2], Amy C. Bennett[2], Christopher V. So[2], Norman A. Bourg[2], Jonathan R. Thompson[3], Sean M. McMahon[1,4] and William J. McShea[2]

[1]*Center for Tropical Forest Science-Forest Global Earth Observatory, Smithsonian Tropical Research Institute, Panama, Republic of Panama, 9100 Panama City Pl; Washington, DC 20521-9100, USA;* [2]*Conservation Ecology Center, Smithsonian Conservation Biology Institute, National Zoological Park, 1500 Remount Rd., Front Royal, VA 22630, USA;* [3]*Harvard Forest, Harvard University, 324 N. Main Street, Petersham, MA 01377, USA; and* [4]*Forest Ecology Group, Smithsonian Environmental Research Center, PO Box 28, Edgewater, MD 21037, USA*

Summary

1. Many morphological, physiological and ecological traits of trees scale with diameter, shaping the structure and function of forest ecosystems. Understanding the mechanistic basis for such scaling relationships is key to understanding forests globally and their role in Earth's changing climate system.

2. Here, we evaluate theoretical predictions for the scaling of nine variables in a mixed-age temperate deciduous forest (CTFS-ForestGEO forest dynamics plot at the Smithsonian Conservation Biology Institute, Virginia, USA) and compare observed scaling parameters to those from other forests world-wide. We examine fifteen species and various environmental conditions.

3. Structural, physiological and ecological traits of trees scaled with stem diameter in a manner that was sometimes consistent with existing theoretical predictions – more commonly with those predicting a range of scaling values than a single universal scaling value.

4. Scaling relationships were variable among species, reflecting substantive ecological differences.

5. Scaling relationships varied considerably with environmental conditions. For instance, the scaling of sap flux density varied with atmospheric moisture demand, and herbivore browsing dramatically influenced stem abundance scaling.

6. Thus, stand-level, time-averaged scaling relationships (e.g., the scaling of diameter growth) are underlain by a diversity of species-level scaling relationships that can vary substantially with fluctuating environmental conditions. In order to use scaling theory to accurately characterize forest ecosystems and predict their responses to global change, it will be critical to develop a more nuanced understanding of both the forces that constrain stand-level scaling and the complexity of scaling variation across species and environmental conditions.

Key-words: allometry, Center for Tropical Forest Science-Forest Global Earth Observatory , ecosystem, global, large forest dynamics plot, metabolic ecology, scaling theory, temperate deciduous forest

Introduction

Numerous structural, physiological and ecological characteristics of trees vary systematically with trunk diameter. These include height, numbers and lengths of branches, crown dimensions, leaf area, stem and root mass, sapwood area, transpiration, woody growth, mortality and stem abundance (e.g. Niklas 1994; Savage *et al.* 2010). Scaling relationships – that is, functions describing the relationship between such traits and tree stem diameter or mass – have broad utility for characterizing the structure and function of forest ecosystems and predicting forest responses to global change. They can be used to estimate whole-ecosystem properties such as biomass, productivity or transpiration

*Correspondence author. E-mail: teixeirak@si.edu

© 2015 The Authors. Functional Ecology © 2015 British Ecological Society

based on the number and size of trees present (e.g. Wullschleger, Hanson & Todd 2001; Mascaro *et al.* 2011). On a practical level, this is quite valuable because tree diameter is one attribute that is consistently measured by forest inventory networks around the world (e.g. Malhi *et al.* 2002; Woudenberg *et al.* 2010 Anderson-Teixeira *et al.* 2015a). Scaling relationships can be incorporated into ecosystem models, thereby helping to predict forest responses and feedbacks to climate change (e.g. Moorcroft, Hurtt & Pacala 2001; Purves & Pacala 2008). Furthermore, scaling relationships can help to characterize how biophysical constraints shape ontogenetic and evolutionary trade-offs and to define the functional basis for physiological and ecological differences among trees of different sizes (Sperry *et al.* 2012; Smith *et al.* 2014). In combination with extensive forest inventory data sets containing diameter measurements, any scaling relationship with sufficient generality to be broadly applicable and sufficient precision to characterize meaningful differences among species and varying environmental conditions could prove invaluable to understanding global forest ecosystems and their role in Earth's changing climate system.

A great deal of attention has focused on the mechanistic basis for scaling of ecological form and function with tree size (Table 1). Scaling relationships can most generally be approximated by a power function:

$$Y = Y_o X^z \qquad \text{eqn 1}$$

Here, Y is the trait of interest, X is a measure of the organism's size (e.g. diameter, mass), Y_o is a scaling factor, and z is an exponent characterizing the magnitude of change in Y with an increase in X. Although other functions sometimes yield better statistical fits for particular variables, power functions can provide baseline approximations of scaling relationships across a wide range of ecological response variables and facilitate scaling across levels of biological organization (e.g. Niklas 1994; Sibly, Brown & Kodric-Brown 2012). One proposed mechanism for such scaling, put forth as part of the metabolic theory of ecology (MTE; Brown *et al.* 2004), is that vascular networks have a fractal structure optimized to maximize the efficiency of resource distribution, leading to universal scaling relationships describing organisms' morphology and metabolism (West, Brown & Enquist 1999a) and that metabolism in turn sets the pace of life, with pervasive effects on ecology (Brown *et al.* 2004; Sibly, Brown & Kodric-Brown 2012). Henceforth, we refer to MTE's predictions for trees and forests as the metabolic scaling theory of forests, MSTF (*sensu* Coomes *et al.* 2012). Within MSTF, particular attention has focused on predicting values for z based on biophysical and biological mechanisms, and scientific debate on this theme has led to a range of predictions as to how various traits should scale with tree size (Table 1, where 'a' predictions are original MSTF predictions). This line of research is essential because a generalizable, mechanistic understanding of scaling in forests is necessary to apply scaling models to novel environmental conditions (e.g. future climates) and to regions where extensive diameter data exist but few other characteristics of the forest are known. However, existing theoretical predictions do not consistently and reliably characterize observed patterns or, by extension, provide sufficient accuracy to predict forest responses to global change. For scaling theory to become more effective at describing the structure and dynamics of forests globally, three broad challenges must be addressed.

To begin with, it is important to understand when and why stand-level patterns observed in forests deviate from theoretical predictions. There are two major reasons why theoretical predictions may deviate from observations. First, underlying assumptions about the structure, physiology or ecology of trees may fail to capture some of the factors that meaningfully influence scaling patterns. The original MSTF predictions describe highly idealized trees and forests (West, Brown & Enquist 1999b; Enquist, West & Brown 2009; West, Enquist & Brown 2009; Savage *et al.* 2010), incorporating a number of simplifying assumptions about plant vascular networks and forest ecology that influence scaling predictions but are not supported by empirical data (e.g. Coomes & Allen 2007; Price *et al.* 2012). Secondly, theoretical predictions that assume constant environmental conditions across tree size classes – as do most original MSTF predictions – will almost inevitably fail to accurately represent scaling relationships in forests where trees of different sizes experience substantially different environmental conditions (Muller-Landau *et al.* 2006a; Poorter *et al.* 2008; Rüger & Condit 2012). Light environment, evaporative demand and leaf traits all vary with height in a canopy, and consequently with tree size (e.g. Roberts, Cabral & Aguiar 1990; Muller-Landau *et al.* 2006a; McDowell *et al.* 2011). Belowground, soil moisture and nutrient availability vary with depth, implying that tree physiology is influenced by rooting depth and size (Meinzer *et al.* 1999). In addition, trees of different sizes are exposed to differential levels of disturbance (*e.g.* more intense exposure to wind for top of canopy trees, greater browsing pressure for understorey individuals). Thus, environmental conditions vary systematically with tree size, which inevitably affects the scaling of form and function with size but is not currently accounted for in most theoretical predictions (Table 1).

Secondly, variability in species-level scaling relationships needs to be characterized, and the factors that drive this variability understood. Species-level (intraspecific) scaling relationships vary among species and may deviate substantially from stand-level (interspecific) scaling relationships characterizing the forest community as a whole (e.g. Price *et al.* 2009; Pretzsch & Dieler 2012). Deviation in species-level scaling relationships from central tendencies, or from stand-level scaling, may be driven by a variety of genetic and environmental factors. For instance, branching symmetry affects the scaling of crown area and light interception (Smith *et al.* 2014). In addition, the scaling of transpiration with tree size should vary with a number of

© 2015 The Authors. Functional Ecology © 2015 British Ecological Society, *Functional Ecology*, **29**, 1587–1602

Table 1. Summary of theoretically predicted diameter-scaling relationships and their consistency with relationships observed at the Smithsonian Conservation Biology Institute (SCBI) and at other sites around the world. Included are studies that provide a mechanistic basis for predicted scaling relationships. When applicable, predicted scaling exponents (*z;* Eqn 1) are listed. Consistency with observed relationships is determined based on whether the predicted z (if any) falls within the 95% CI of the observed relationships, and does not necessarily imply support for the proposed mechanisms.

					Consistency with data*		
Variable	Prediction	Predicted z	Basis	References	SCBI: stand-level	Global: stand-level†	SCBI: species-level
1. Tree Height (h; m)	1a	0·67	Mechanical stability (safety from buckling)	McMahon & Kronauer (1976); West, Brown & Enquist (1999b)	1/1	*0/1*	2/2
	1b	≥0·67‡	Growth & hydraulic constraints	Niklas & Spatz (2004)	1/1	*1/2*	2/2
	1c	(<0·67)§	A variety of mechanisms other than mechanical stability may limit h of large-diameter trees	Ryan & Yoder (1997); Becker, Meinzer & Wullschleger (2000); Koch *et al.* 2004; Banin *et al.* (2012)	1/1	*2/2*	2/2
2. Crown Area (A_c; m^2)	2a	1·33	Symmetrical self-similar branching.	West, Enquist & Brown (2009)	0/1	*1/3*	2/2
	2b	–	Relaxation of unrealistic symmetrical self-similar branching assumption leads to a diversity of z_{Ac} s.	Mäkelä & Valentine (2006); Smith *et al.* (2014)	–	–	–
3. Crown Volume (V_c; m^3)	3a	2	Proportional to number of leaves (scaling as $z = 2$), assuming $z_{Ac} = 1{\cdot}33$.	West, Enquist & Brown (2009)	0/1	*0/0*	2/2
	3b	<2	Based on scaling of V_c with h ($z < 3$) and h –DBH scaling with $z_h = 0{\cdot}67$, V_c should scale with DBH with $z_{Vc} < 2$.	Simini *et al.* (2010); Anfodillo *et al.* (2013)	1/1	1/1	2/2
	3c	–	Relaxation of unrealistic symmetrical self-similar branching assumption leads to a diversity of crown volume scaling exponents.	Mäkelä & Valentine (2006); Smith *et al.* (2014)	–	–	–
4. Sapwood area (A_s; cm^2)	4a	2	$A_s : A_b$ (basal area) invariant with DBH.	Savage *et al.* (2010)	0/1¶	*0/0*	8/15
	4b	1–2	Geometric constraints, assuming that sapwood thickness does not decrease with increasing diameter.	Sperry *et al.* (2012)	1/1	*3/3*	14/15
5. Peak Sap Flux Density ($F_{d,max}$; m h^{-1})	5a	0	None. (Empirical evidence.)	West, Brown & Enquist (1999b); Savage *et al.* (2010)	1/1	0/1	1/2
6. Peak Transpiration (F_{max} L hr^{-1})	6a	2	Product of sapwood area (with $z_{As} = 2$) and peak sap flux density (with $z_{Fd,max} = 0$). Alternatively, transpiration ∝ number of leaves ∝ crown volume (with $z_{Vc} = 2$).	West, Enquist & Brown (2009); Savage *et al.* (2010)	0/1	0/0	1/2
	6b	0·7–1·9	Numerical model incorporating empirical observations of relevant parameters.	Sperry *et al.* (2012)	1/1	0/0	2/2
	6c	<2**	Numerical model incorporating empirical observations of non-symmetrical branching.	Smith *et al.* (2014)	1/1	0/0	2/2
7. Diameter Growth Rate (G_d; mm $year^{-1}$)	7a	0·33	Assumes annual C allocation to growth ∝ annual C fixation ∝ daily C fixation ∝ daily transpiration ∝ peak transpiration (with $z_{Fmax} = 2$).	Enquist & Niklas (2001); West, Enquist & Brown (2009)	0/3††	1/13	2/15‡‡
	7b	>0·33	In closed-canopy forests, scaling should be steeper than the above prediction because large trees receive more light.	Muller-Landau *et al.* (2006a); Coomes & Allen (2009); Coomes, Lines & Allen (2011); Rüger & Condit (2012)	3/3††	12/13	15/15‡‡

Table 1 (continued)

Variable	Prediction	Predicted z	Basis	References	Consistency with data*		
					SCBI: stand-level	Global: stand-level†	SCBI: species-level
8. Mortality Rate (M; % year^{-1})	8a	−0·67	Assumes that M is proportional to mass-specific biomass growth rate ($z_M = z_{Gd} - 1$, where $z_{Gd} = 0{\cdot}33$ as in prediction 7a).	Brown *et al.* (2004); West, Enquist & Brown (2009)	0/1	0/13	11/15
	8b	[$z_{Gd} - 1$]	Assumes that M is proportional to mass-specific biomass growth rate ($z_M = z_{Gd} - 1$, where z_{Gd} is measured empirically).	Brown *et al.* (2004)	1/1	2/13	9/15
	8c	–	Competitive thinning and exogenous disturbances jointly affect scaling, commonly resulting in U-shaped mortality curves and resulting in a variety of scaling exponents.	Coomes *et al.* (2003); Coomes & Allen (2007)	–	–	–
9. Abundance (N; n ha^{-1})	9a	−2	Energy equivalence (equal population energy use across size classes)	Enquist & Niklas (2001); West, Enquist & Brown (2009)	0/1	1/31	0/15
	9b	–	Abundance distributions are better described by demographic equilibrium models that incorporate observed scaling of growth and mortality, resulting in a variety of scaling exponents.	Muller-Landau *et al.* (2006b); Coomes & Allen (2007)	–	–	–

*Numbers indicate [n scaling relationships for which the observed scaling was consistent with prediction]/[n scaling relationships examined].
†Many studies reviewed reported z but not its 95% CI and are therefore excluded from this count, except in cases where reported z falls within a predicted range of values. Cases where some records were excluded for lack of 95%CI are italicized.
‡Dependent on diameter range, converging to 0·67 for large trees.
§This value is not specifically predicted by the references listed, but would be the logical conclusion of other mechanisms limiting h beyond the limits imposed by mechanical stability.
¶This prediction is consistent with observations from diffuse porous species.
**For the scenario considered in this paper, which was one of the highest-exponent scenarios of Sperry *et al.* (2012), exponent ranged from 1·81 to 1·96 (highest for small trees).
††Measured using three approaches (5-year growth from census data, dendrometer bands, and growth increments from cores).
‡‡Refers to 5-year growth data.

© 2015 The Authors. Functional Ecology © 2015 British Ecological Society, *Functional Ecology*, **29**, 1587–1602

functional traits including xylem anatomy, the sapwood area to basal area ratio, sapwood capacitance (i.e., ability to store water), leaf hydraulic conductance, bark thickness and branching symmetry (Meinzer *et al*. 2003; Sperry *et al*. 2012; Smith *et al*. 2014). Understanding diversity in species-level scaling relationships will be important to characterizing how various taxa contribute to stand-level scaling relationships.

Thirdly, it is important to understand how scaling relationships are influenced by variation in environmental conditions, be it temporal (e.g. in micrometeorological conditions) or spatial (e.g. in climate, soils, herbivore population density). Forests are subject to environmental variation in space and time, and many environmental drivers may interact with tree size such that the parameters of scaling relationships also vary. For instance, trees of different sizes have responded differently to drought and to CO_2 fertilization and warming experiments (e.g. Phillips *et al*. 2010; Anderson-Teixeira *et al*. 2013). Variables known to affect scaling relationships also vary through space; for example, tree heights and crown dimensions vary with aridity and elevation (Lines *et al*. 2012). Thus, the parameters of scaling relationships should vary through time and space with environmental variables – an expectation that generally is not addressed by most current scaling theory (Table 1). In the present era of global change, understanding interactions between environmental conditions and scaling relationships may provide valuable insights into mechanisms underlying changes in forest structure, composition and function.

Here, using a temperate broadleaf deciduous forest in Virginia, USA, as a study system and including a review of observations from forests globally, we characterize the scaling of tree height, crown dimensions, sapwood area, sap flow velocity, transpiration, diameter growth, mortality and stem abundance to address three questions:

1. *How well is the scaling of tree form and function within a closed-canopy forest described by existing theoretical predictions?* This question is addressed by comparing theoretical predictions (Table 1) with observed stand-level scaling relationships for nine response variables. In addition, we evaluate theoretical predictions against scaling relationships observed in forests globally.
2. *How commonly, and by how much, do species-level scaling relationships deviate from theoretical predictions and from stand-level scaling relationships describing the forest community as a whole?* This is addressed through comparison of species-level scaling relationships for up to 15 species (depending on variable) with theoretical predictions (Table 1) and stand-level scaling relationships.
3. *How does the scaling of physiological and ecological characteristics with tree size vary with environmental conditions in time and space?* This is addressed by comparing scaling relationships observed under different weather conditions and in areas with different herbivore browsing pressures.

Materials and methods

STUDY SITE

Research was conducted in the Center for Tropical Forest Science (CTFS)-Forest Global Earth Observatory (ForestGEO) large forest dynamics plot located at the Smithsonian Conservation Biology Institute (SCBI) in Front Royal, VA, USA (38°53′36·6″ N, 78°08′43·4″ W; (Bourg *et al*. 2013; Anderson-Teixeira *et al*. 2015a). The plot is 25·6 ha (400 m × 640 m), with elevation ranging from 273 to 338 m.a.s.l. (mean 302 m). Mean annual temperature and precipitation from 2010 to 2013 were 12·9 °C and 1001 mm, respectively. The SCBI site is a mature secondary eastern mixed deciduous forest, with the majority of canopy trees having established around 1900 (Bourg *et al*. 2013). In total, the plot contains 62 species of woody plants with at least one stem of DBH ≥1 cm. The 15 most abundant canopy species include *Carya* spp. (hickories; 4 species), *Liriodendron tulipifera* L. (tulip poplar), *Quercus* spp. (oaks; 4 species), *Nyssa sylvatica* Marshall (black gum), *Fraxinus americana* L. (white ash), *Fagus grandifolia* Ehrh. (American beech), *Ulmus rubra* Muhl. (slippery elm), *Acer rubrum* L. (red maple) and *Juglans nigra* L. (black walnut), in total accounting for an estimated 99·2% of live biomass (based on 2008 census; Bourg *et al*. 2013; see Appendix S1 and Table S1 in Supporting Information). Four hectares of the plot have been fenced to exclude *Odocoileus virginianus* Zimmerman (white-tailed deer) since 1990, leading to taller tree seedlings and greater sapling density within the exclosure (McGarvey *et al*. 2013).

MEASUREMENTS

We measured tree height, crown area, crown depth (*i.e*. distance from top to bottom of crown; see Appendix S1), bark thickness, sapwood (hydroactive xylem) depth, sap flux density (*i.e*. rate of water movement in xylem), annual stem diameter growth increments from tree cores, seasonal stem diameter growth (measured using dendrometer bands), 5-year stem diameter growth, mortality and stem abundance on trees spanning a large range of diameter at breast height (DBH; 1–152 cm). These measurements are summarized briefly below, and methods are detailed in Appendix S1. Species, DBH size range and sample sizes for all measurements are also given in the Supplementary Information (Tables S2–S7).

Censuses were conducted in 2008 and 2013 using standard CTFS-ForestGEO protocol (Condit 1998). Specifically, all stems of DBH ≥1 cm were mapped, tagged, identified to species, classified as live or dead and measured in DBH (for 2013, n = 45 613 live stems). These data were used for calculations of stem abundance (2013), 5-year diameter growth (2008–2013), and mortality (2008–2013).

Several additional variables were measured on subsets of trees randomly sampled throughout the plot and representing the range of tree sizes (Appendix S1). These variables were tree height (n = 290), crown area (n = 60), crown depth (n = 60), bark thickness (n = 119), sapwood thickness (n = 681), annual growth increments from tree cores (n = 564) and seasonal diameter growth (n = 499). Tree cores collected in 2010 (n = 681) were used to estimate sapwood depth based on colour differences between sapwood and heartwood and to quantify annual growth increments. From the raw ring widths, we calculated mean annual growth increment for the years 1999–2009. Seasonal diameter growth was measured using metal dendrometer bands according to CTFS-ForestGEO protocols (Anderson-Teixeira *et al*. 2015a).

Sap flux density (F_d) was monitored from 18 July–23 September 2013 (n = 24 trees) and from 1 June–14 September 2014 (n = 31 trees) using the Granier method (Granier 1985) in two 15-m-radius subplots, which fell at the low end of the elevation range within the SCBI plot (<300 m), had minimal relief and were

relatively mesic (within 5 m elevation of a perennial stream). Subplots were selected to minimize water limitation and to contain the maximum possible size range for two of the 15 most dominant canopy species, *F. grandifolia* and *L. tulipifera*. All trees >5 cm DBH within these plots were instrumented with sap flow probes and dendrometer bands, and their height and crown dimensions were measured. Whole-tree transpiration (L h^{-1}) was calculated based on F_d and sapwood area, with a correction for radial patterns in F_d (see Appendix S1).

A meteorological station in a field adjacent to the forest plot measured temperature, humidity, wind speed and direction, precipitation and solar radiation at 5-min intervals (see Appendix S1 for details).

DATA ANALYSES

Stand-level scaling relationships were fit to data from all species combined. Species-level scaling relationships were calculated for two focal species for which all variables were measured (*F. grandifolia* and *L. tulipifera*) and, when feasible, for all of the 15 most common overstorey species (Table S1). We further examined several instances of scaling relationships under different environmental conditions: (i) scaling of peak sap flux density in *F. grandifolia* under low and high atmospheric moisture demand; (ii) scaling of the ratio of growth increment during a normal year (1985; Palmer Drought Severity Index, PDSI = −0·866) to a drought year 1986 (driest year within the last thirty years for Virginia; PDSI = −3·356; National Climatic Data Center 2013); (iii) scaling of stem abundance under areas of high and minimal deer browsing pressure.

Because the goal of this analysis was to compare empirical observations with theoretical predictions expressed as power functions (eq. 1), all relationships were fit with power functions – even for variables for which other functions were known to provide a statistically better fit (e.g. Coomes *et al.* 2003; Muller-Landau *et al.* 2006b; Banin *et al.* 2012). With the exception of the tree size distribution (see below), power functions were fit using ordinary least squares (OLS) regression on log-transformed data (White *et al.* 2012). OLS regression was favoured based on our assessment that error in DBH measurements is relatively small compared with error in the response variables. Power function abundance distributions were fit using maximum likelihood as in Muller-Landau *et al.* (2006b) (detailed in Appendix S1).

The focus of most theoretical predictions – along with that of this study – is on the exponent z; specific predictions for the scaling factor Y_0 (eq. 1) are neither generated by most theoretical studies nor compared here. Consistency of observations with theoretical predictions was assessed based on whether theoretically predicted zs, if any, fell within 95% CIs of empirical scaling relationships. Some theoretical predictions are based on numerical models predicting variation in z as a function of a variety of branching patterns or functional traits (e.g. predictions 2b, 3b, 6b, 6c; Table 1). In these cases, we tested only whether the 95% CI of the observed z overlapped with the predicted range; thus, our analysis provides only a first-order test of these predictions. For comparison of species-level and stand-level scaling exponents, we used a two-sided t-test to assess the significance of differences between zs.

COMPARISON WITH FORESTS GLOBALLY

To place our results in the context of forests globally, we compiled data on scaling exponents from closed-canopy broadleaf forests world-wide. We conducted a non-comprehensive but systematic search for relevant studies (detailed in Appendix S1). Criteria for inclusion were (i) data came from a single site and (ii) data were fit with power functions in the form of Eq.1, and the scaling exponent z reported. Again, consistency with theoretical predictions was assessed based on whether theoretically predicted zs, if any, fell within reported 95% CIs (when reported).

Results

All of the variables examined, with the exception of sap flux density, varied significantly (at $P < 0{\cdot}05$) with DBH for stand-level scaling relationships and for most species-level scaling relationships (Fig. 1; Tables S2–S7). A power function (eq. 1) often provided an appropriate fit; however, there were some significant nonlinearities on the log–log scale, particularly in the cases of 5-year growth and stem abundance scaling, and scaling relationships were quite variable in terms of the amount of observed variation explained (Fig. 1; Tables S2–S7). Consistent with the primary focus of MSTF, our analysis focused exclusively on power function fits, and our presentation of results below focuses on comparison of the scaling exponent, z, without consideration of the intercept, Y_0 (Eq. 1). Henceforth, we refer to comparisons where the observed z is closer to zero than the predicted z as scaling 'less steeply' (e.g. Fig. 1h, i, j) and those where the absolute value of the observed z is greater than that of the predicted z as scaling 'more steeply' (e.g., Fig. 1b, k, l). We use the sign convention that a z subscripted with a variable symbol refers to the scaling of that variable with DBH (*i.e.* z_Y refers to the scaling of Y).

STAND-LEVEL SCALING VS. THEORETICAL PREDICTIONS

Generally speaking, stand-level scaling relationships at SCBI (Fig. 1; Tables S2–S7) and other forests around the world (Fig. 2; Table S8) occasionally matched – but more often differed significantly from – the original theoretical predictions of MSTF ('a' predictions, Table 1; Fig. 2). Observed relationships were usually consistent with theory predicting a wider range of potential exponents (Table 1). Specifics follow.

The scaling of tree height (h) at SCBI (Figs 1a and 2) did not provide basis for rejection of any of the three theoretical predictions for the scaling of tree height (predictions 1a-1c; Table 1); specifically, the theoretically predicted z_h values of ≥0·67 (predictions 1a, 1b) and <0·67 (prediction 1c) fell within the 95% CI for the observed z_h ($z_h = 0{\cdot}704 \pm 0{\cdot}039$; $R^2 = 0{\cdot}85$). In other broadleaved forests around the world, z_h was relatively close to the original MSTF prediction of $z_h = 0{\cdot}67$; the absolute difference was <0·1 for all three stand-level relationships reviewed, although z_h was significantly lower than 0·67 for a forest in Panama (Fig. 2; Table S8; Muller-Landau *et al.* 2006a).

At SCBI, crown area and volume (A_c and V_c, respectively) scaled less steeply than originally predicted by MSTF. Specifically, A_c scaled less steeply

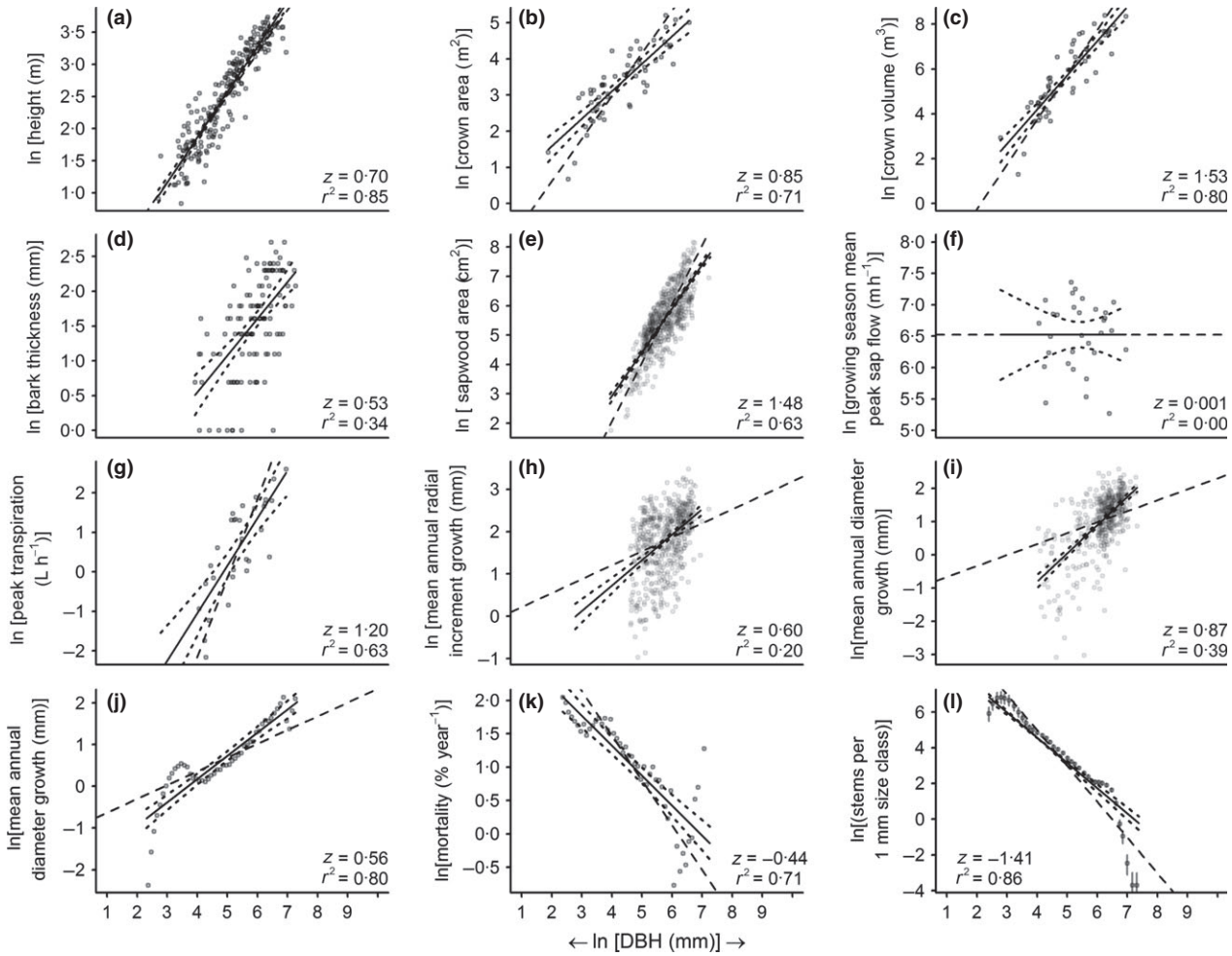

Fig. 1. Comparison of empirically observed scaling relationships and theoretically predicted scaling exponents. Shown are the relationships between DBH and (a) tree height; (b) crown area; (c) crown volume; (d) bark thickness (no theoretically predicted z); (e) sapwood area; (f) median daily maximum sap flux density for the 2014 growing season; (g) median daily maximum sap flow (transpiration) for the 2014 growing season; (h) mean radial growth increment (from tree cores); (i) average annual diameter growth from dendrometer bands (2008–2014); (j) diameter growth over 5 years (2008–2013); (k) mortality over 5 years (2008–2013); and (l) stem abundance in 2013 (including 95% confidence intervals for each size class). Solid and dotted lines indicate observed scaling relationships and their 95% CIs, respectively (Tables S2–S7); dashed lines represent those theoretically predicted scaling relationships that predict a specific value for z ('a' predictions in Table 1). For visualization of theoretical predictions, which are concerned with slope (z) but not intercept ($\ln[Y_0]$), Y_0 was scaled such that predicted Y was equal to the mean observed Y at the midpoint DBH. All relationships are statistically significant at $P < 0{\cdot}001$ with the exception of sap flux density ($P = 0{\cdot}97$).

($z_{Ac} = 0{\cdot}853 \pm 0{\cdot}147$; $R^2 = 0{\cdot}71$; Fig. 1b) than the original MSTF prediction of $z_{Ac} = 1{\cdot}33$ (prediction 2a; Table 1; Fig. 2), a finding consistent with the theoretical prediction of a diversity of z_{Ac}s (prediction 2b). Similarly, V_c scaled less steeply ($z_{Vc} = 1{\cdot}528 \pm 0{\cdot}206$; $R^2 = 0{\cdot}80$; Fig. 1c) than the theoretical prediction of $z_{Vc} = 2$ (prediction 3a; Table 1; Fig. 2), being consistent with theoretical predictions of $z_{Vc} < 2$ (prediction 3b) or a diversity of scaling exponents (prediction 3c). At other sites throughout the world, both A_c (4 scaling relationships from 3 sites) and V_c (1 scaling relationship) scaled more steeply than at SCBI and were sometimes close to the original MSTF predictions of $z_{Ac} = 1{\cdot}33$ and $z_{Vc} = 2$ (Table 1; Fig. 2; Table S8).

The scaling of sapwood area (A_s) sometimes aligned with the specific original prediction of MSTF assuming constant A_s: A_b, where A_b is basal area ($z_{As} = 2$; prediction 4a; Table 1), but was generally better described by subsequent theory recognizing a wider range of potential exponents associated with declining A_S: A_B ($1 \leq z_{As} \leq 2$; prediction 4b). Specifically, A_s scaled as $z_{As} = 1{\cdot}490 \pm 0{\cdot}086$ ($R^2 = 0{\cdot}63$; Fig. 1e), which was significantly less steep than the prediction that $z_{As} = 2$ (prediction 4a), but consistent with the prediction that $1 \leq z_{As} \leq 2$ (prediction 4b). The same held true for ring porous species as a group ($z_{As} = 1{\cdot}404 \pm 0{\cdot}102$; $R^2 = 0{\cdot}60$). In contrast, for diffuse porous species, which generally had higher A_s: A_b than ring porous species (Table S3), the 95% CI for z_{As} included 2 ($z_{As} = 1{\cdot}908 \pm 0{\cdot}097$; $R^2 = 0{\cdot}89$), providing no basis for rejection of assumptions of either constant or declining A_s: A_b with increases in DBH (predictions 4a and 4b; Table 1). In forests throughout the world (Fig. 2a;

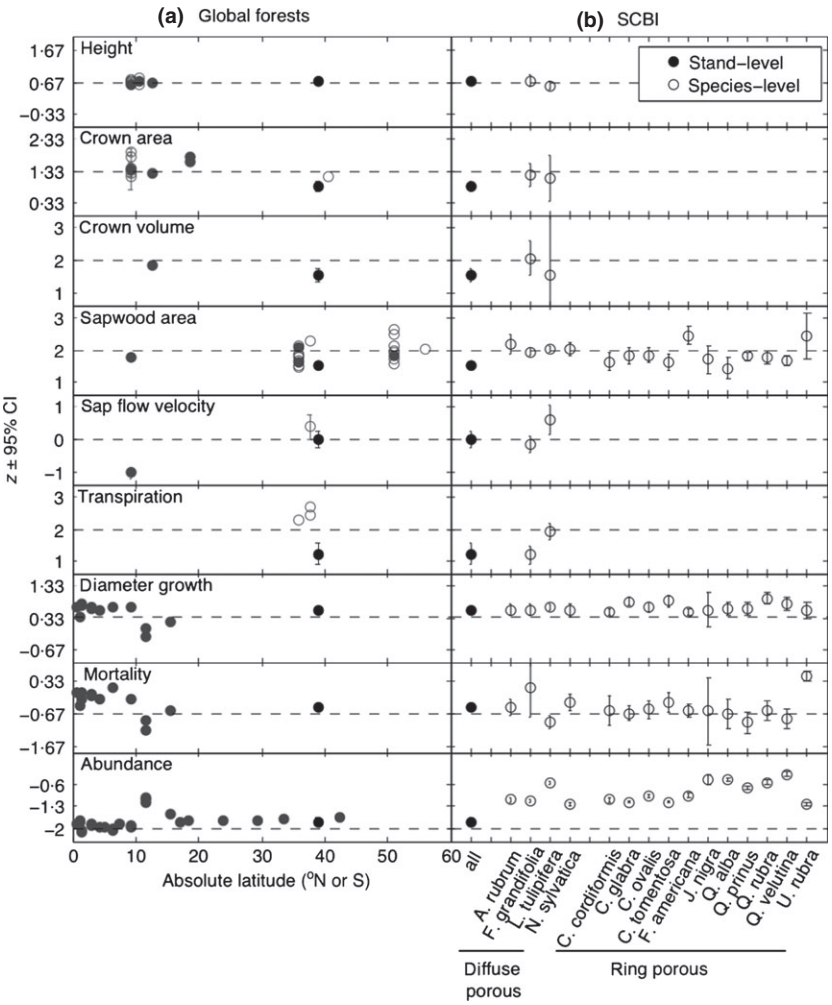

Fig. 2. Comparison of scaling exponents (z) observed at SCBI (black symbols) and other closed-canopy broadleaf forests world-wide (grey symbols) with theoretical predictions that give specific values for z ('a' predictions in Table 1; dashed lines). (a) Stand-level allometries for forests around the world (Table S8) plotted as a function of latitude; (b) Stand-level and species-level allometries at SCBI. Error bars (not always visible) represent 95% CI (see Table S8 for 95% CIs). Y-axes are scaled such that all have a range of 2·4, thereby allowing comparison across variables. Diameter growth scaling exponents for SCBI are for 5-year growth data.

Table S8), the scaling of A_s was variable, with a tendency for z_{As} to be less than or equal to the original MSTF prediction of $z_{As} = 2$ (prediction 4a; Table 1) – results that generally support prediction 4b (Table 1).

Peak sap flux velocity ($F_{d,max}$)– that is, maximum daily water velocity (m h^{-1})– did not vary with tree size in 2013 ($n = 24$; $z_{Fd,max} = 0{\cdot}048 \pm 0{\cdot}212$, $R^2 = 0{\cdot}01$; $P = 0{\cdot}66$) or 2014 ($n = 31$; $z_{Fd,max} = 0{\cdot}001 \pm 0{\cdot}251$, $R^2 < 0{\cdot}01$; $P = 0{\cdot}99$; Table S4). This matched the MSTF assumption that $z_{Fd,max}$ is independent of DBH (assumption 5a, Table 1; Figs 1f and 2). Similarly, total daily sap flux velocity ($F_{d,day}$; m day^{-1}) was independent of DBH in both 2013 ($z_{Fd,day} = 0{\cdot}230 \pm 0{\cdot}236$; $R^2 = 0{\cdot}14$; $P = 0{\cdot}07$) and 2014 ($z_{Fd,day} = 0{\cdot}203 \pm 0{\cdot}256$; $R^2 = 0{\cdot}08$; $P = 0{\cdot}13$). When species were separated into diffuse porous and ring porous groups, $z_{Fd,max}$ and $z_{Fd,day}$ were generally independent of tree size (Table S4), with the exception that $z_{Fd,day}$ was significantly greater than zero for diffuse porous species in 2014 ($n = 25$, $z_{Fd,day} = 0{\cdot}284 \pm 0{\cdot}257$; $R^2 = 0{\cdot}17$; $P = 0{\cdot}04$). For forests globally, we are aware of only one other stand-level scaling relationship for $F_{d,max}$: a significantly negative $z_{Fd,max}$ ($-1{\cdot}038 \pm 0{\cdot}166$) was observed in Panama (Meinzer, Goldstein & Andrade 2001), differing substantially from both prediction 5a (Table 1) and observations at SCBI (Fig. 2a; Table S8). In contrast, a positive species-level scaling relationship has also been observed ($z_{Fd,max} = 0{\cdot}398 \pm 0{\cdot}376$ in Australia; Table S8; Vertessy *et al.* 1995).

Peak transpiration (F_{max})– that is, the total rate of water transport integrated over A_s (L h^{-1})– increased less steeply with DBH than expected based on the original MSTF model predicting that V_c and A_s scale as DBH^2 (prediction 6a; Table 1; Figs 1g and 2); specifically, z_{Fmax} was significantly less than the predicted $z_{Fmax} = 2$ in both 2013 ($z_{Fmax} = 1{\cdot}374 \pm 0{\cdot}312$; $R^2 = 0{\cdot}77$) and 2014 ($z_{Fmax} = 1{\cdot}204 \pm 0{\cdot}338$; $R^2 = 0{\cdot}63$). The same held true of transpiration scaling in diffuse porous species only, while wide 95%CIs for ring porous species included the theoretically predicted $z_{Fmax} = 2$ (Table S4). These results fall within the wide range of potential values for z_{Fmax} described by models incorporating observed variation in the scaling of V_c and A_s (predictions 6b and 6c; Table 1). The scaling of daily transpiration (F_{day}) was somewhat steeper than that of F_{max} in both 2013 ($z_{Fday} = 1{\cdot}537 \pm 0{\cdot}313$; $R^2 = 0{\cdot}80$) and 2014 ($z_{Fday} = 1{\cdot}409 \pm 0{\cdot}340$; $R^2 = 0{\cdot}69$; Table S4). We are not aware of any other studies characterizing stand-level scaling of F_{max}; however, studies in Tennessee, USA, and Victoria, Australia estimated z_{Fmax} values greater than

the MSTF prediction of $z_{F\max} = 2$ (no CIs given; Fig. 2a; Table S8).

Annual diameter growth (G_d) generally scaled more steeply with DBH than expected based on assumptions that tree mass growth rate is proportional to transpiration across the DBH range (prediction 7a; Table 1; Table S5). At SCBI, G_d was measured using three methods covering different time-scales and sets of trees (Appendix S1): increment growth cores ($n = 564$, 9 species; Fig. 1h), dendrometer bands ($n = 499$, 12 species; Fig. 1i) and a 5-year census ($n = 45\,613$, 62 species; Fig. 1j). Despite these differences, in all cases, G_d scaled more steeply than the original MSTF prediction of $z_{Gd} = 0{\cdot}33$ (prediction 7a). Specifically, scaling of core growth increments gave $z_{Gd} = 0{\cdot}599 \pm 0{\cdot}098$ ($R^2 = 0{\cdot}20$), dendrometer bands gave $z_{Gd} = 0{\cdot}870 \pm 0{\cdot}089$ ($R^2 = 0{\cdot}39$), and the 5-year census gave $z_{Gd} = 0{\cdot}557 \pm 0{\cdot}079$ ($n = 50$ size bins; $R^2 = 0{\cdot}80$). These results supported the prediction that scaling should be steeper than the original MSTF prediction of $z_{Gd} = 0{\cdot}33$ (prediction 7b; Table 1). There was significant nonlinearity to the scaling of growth estimates derived from 5-year census data (Fig. 1j), but exclusion of the lower size classes where this nonlinearity occurs would not alter the conclusion that $z_{Gd} > 0{\cdot}33$. Similarly, in tropical forests globally (Fig. 2a; Table S8; Muller-Landau *et al.* 2006a), the majority of observed scaling relationships had $z_{Gd} > 0{\cdot}33$ (6 of 9 sites, including 3 sites with two census periods). However, one site did not differ significantly from $z_{Gd} = 0{\cdot}33$ (La Planada, Colombia), and two sites had $z_{Gd} < 0{\cdot}33$ (two census periods in Mudumalai, India and one in Huai Kha Khaeng, Thailand; Table S8).

Average annual mortality rate (M; % year^{-1}) generally scaled less steeply with DBH than expected based on the original MSTF prediction (8a, Table 1; predicted $z_M = -0{\cdot}67$), being more consistent with alternative predictions (8b and 8c; Table 1). At SCBI, M (from 2008 to 2013) had a scaling exponent of $z_M = -0{\cdot}446 \pm 0{\cdot}084$ ($R^2 = 0{\cdot}72$; Fig. 1k; Table S6). This scaling relationship was consistent with prediction 8b – a modification of the original MSTF prediction that retains the assumption that M scales as the inverse of biomass growth rate but drops the assumption that $z_{Gd} = 0{\cdot}33$. Basing the prediction for z_M on the observed z_{Gd} for 5-year growth, the predicted value should be $z_M = z_{Gd} - 1 = -0{\cdot}42$ – a value that does fall within the confidence intervals for mortality scaling observed here, supporting prediction 8b (Table 1). Prediction 8c does not specify any expected values for z_M, but consistent with this prediction, mortality rate did not decrease continuously with tree size; rather, it increased in some of the largest size classes (Fig. 1k). In other forests around the world (all tropical; Fig. 2a; Table S8; Muller-Landau *et al.* 2006a), the majority of observed scaling relationships had $z_M > -0{\cdot}67$ (8 of 9 sites, including 3 with two census periods), and only one site had $z_M < -0{\cdot}67$ (Mudumalai, India; two census periods). At these sites, observed scaling conformed to prediction 8b ($z_M = z_{Gd} - 1$) in only two of 13 instances. U-shaped patterns were observed at many of these sites (Muller-Landau *et al.* 2006a), supporting prediction 8c.

Finally, stem abundance (N; n live stems in the plot, binned into 0·1 cm size bins) generally scaled less steeply with DBH than expected based on the original MSTF prediction ($z_N = -2$; prediction 9a, Table 1; Fig. 1l). At SCBI, scaling was significantly less steep than theoretically predicted ($z_N = -1{\cdot}787$; 95% CI: $-1{\cdot}887$, $-1{\cdot}666$; $R^2 = 0{\cdot}89$). Moreover, stem densities deviated substantially from predictions at the low and high ends of the size spectrum (Fig. 1l). For other forests globally (Fig. 2a; Table S8), most forests had $z_N > -2$ (25 censuses at 15 sites), whereas three sites had $z_N \leq -2$ (1 census with $z_N \leq -2$; 5 censuses at 3 sites with $z_N < -2$). As at SCBI, these stem abundance distributions typically deviated substantially from a power-law fit, being convex downward on log–log axes (Muller-Landau *et al.* 2006b; Lai *et al.* 2013).

SPECIES-LEVEL SCALING

Of the 84 species-level scaling relationships quantified for SCBI (i.e. species-variable combinations; Tables S2–S7), 39 differed significantly from the stand-level relationship in the value of z (Table 2; Fig. 2b). For two of the traits examined (25 of these 39 instances), the mean z of species-level allometries differed by more than 0·3 from the z of the stand-level allometry – a very substantial difference for an exponent. First, stand-level scaling of sapwood area tended to be less steep than species-level z-values (average difference = 0·4; significant difference for 10/15 species) – an artefact of fitting a single scaling relationship to

Table 2. Summary of differences between stand-level and species-level scaling exponent differences observed at SCBI.

Trait	n species deviating significantly from stand-level z*/n species†	Species-level z - stand-level z‡	
		Mean	Max§
Tree Height	1/2	−0·07	−0·14
Crown Area	0/2	0·29	**0·35**
Crown Volume	0/2	0·28	**0·54**
Sapwood Area	**10/15**	**0·40**	**0·97**
Peak Sap Flux Density	1/2	0·15	0·55
Peak Transpiration	1/2	0·21	0·58
Diameter Growth Rate- dendrometer bands	3/12	−0·01	**1·73**
Diameter Growth Rate- cores	**2/2**	0·09	**0·57**
Diameter Growth Rate- 5 year census	4/15	0·08	**0·37**
Mortality Rate	2/15	−0·04	**0·95**
Stem abundance	**15/15**	**0·92**	**1·51**

*Bold indicates that >50% of the species deviated significantly.
†Refers to species for which species-level allometry was analysed.
‡Bold indicates a difference >0·3.
§Refers to greatest absolute difference.

combined data from species that vary in sapwood: basal area (or Y_0 in eq. 1; Fig. 3). Secondly, stem abundance scaling relationships for the individual species considered here had less steep scaling relationships than the community as a whole (average difference = 0·92; significant difference for all 15 species) – a phenomenon driven by relatively low stem abundance of these canopy species in the understorey and consequent poor fits by a power function.

In addition, there were 14 instances (17% of those examined) where species-level scaling relationships of individual species deviated significantly from stand-level relationships (Table 2; Fig. 2b), indicating ecological differences. For example, *F. grandifolia* (Fig. 4), *Liriodendron tulipifera* and *Ulmus rubra* all had multiple anomalous scaling relationships. *F. grandifolia* differed from other species in several ways: (i) much less steep scaling of height to crown base (z = 0·22 compared to z = 0·68 for all species; Fig. 4a) resulting in greater crown volume than other trees of similar size (higher Y_o for V_c; Table S2); (ii) sapwood area was greater and scaled more steeply (Fig. 3; Table S3); (iii) both sap flow velocity and transpiration had a non-significant tendency to be higher, particularly in small trees (Table S4); (iv) diameter growth generally scaled less steeply (Fig. 4b; Table S5); (v) the ratio of growth in a dry versus normal had a decreasing tendency (P = 0·08) with DBH, whereas in other species, it increased (P < 0·001; Fig. 4c; Table S5). *L. tulipifera* differed from other species in that it had (i) steeper scaling of sapwood area (Fig. 3; Table S3); (ii) significantly positive scaling of sap flux density and steeper scaling of transpiration in 2014 (Table S4); (iii) significantly steeper scaling of diameter growth based on both cores and dendrometer bands (but not 5-year growth; Table S5); (iv) steeper scaling of mortality rate (Fig. 2b; Table S6); and (5) less steep scaling of stem abundance (Fig. 2b; Table S7). *U. rubra* had an anomalously positive scaling of mortality rate (Fig. 2b; Table S7), along with 52% mortality from 2008 to 2013.

Of the 84 species-level scaling relationships quantified for SCBI, 33 differed in terms of their consistency with original MSTF predictions (Table 1, Fig. 2b). In 22 of these instances, the species-level z did not differ significantly from the stand-level z, but a wider 95% CI included the theoretical prediction for z that fell outside the 95% CI for the stand-level relationship (Table 1; Fig. 2b). This was the case for the scaling of crown area and volume for *L. tulipifera* and *F. grandifolia,* sapwood area for *Juglans nigra*, 5-year diameter growth for *J. nigra* and *U. rubra*, dendrometer band growth for 4/12 species, and mortality rate for 11/15 species (Fig. 2; Tables S2, S3, S5, S6). In 11 instances, species-level scaling differed significantly from stand-level scaling and also differed in terms of consistency with original MSTF predictions. Seven of these instances were for the scaling of sapwood area; for these species, species-level scaling differed significantly from stand-level scaling (z_{As} <2) and the 95%CIs included the MSTF prediction of z_{As} = 2 (prediction 4a, Table 1; Figs 2 and 3; Table S3). In addition, in 2014, the scaling of peak sap flux density and transpiration was steeper for *L. tulipifera* than for the stand on average, such that, contrary to stand-level

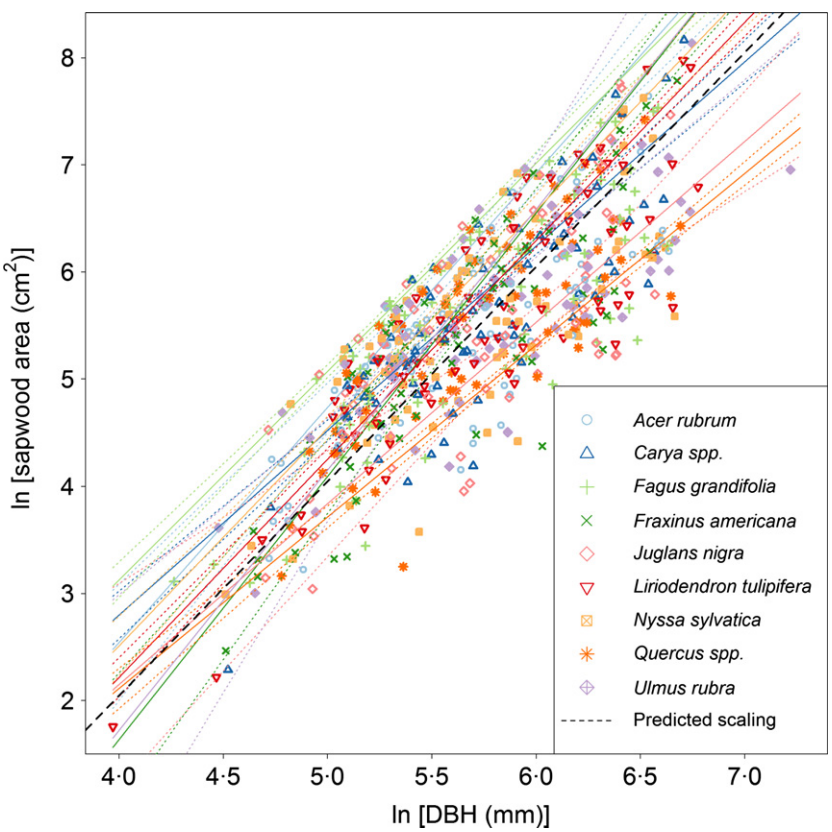

Fig. 3. Scaling of sapwood area with tree diameter varies across species. Shown are relationships for 15 species (grouped by genera) at SCBI, with solid and dotted lines indicating observed species- or genera-level scaling relationships and their 95% CIs, respectively. Black dashed line represents theoretically prediction 4a (Table 1) with Y_0 was scaled such that predicted Y was equal to the mean observed Y at the midpoint DBH. Equations for species-level scaling relationships are given in Table S3.

results, the MTFS assumption that $z_{Fd,max} = 0$ (5a, Table 1) was rejected ($z_{Fd,max} = 0{\cdot}632 \pm 0{\cdot}456$; $R^2 = 0{\cdot}55$; $P = 0{\cdot}04$), while the prediction that $z_{Fmax} = 2$ (6a, Table 1) was not rejected ($z_{Fmax} = 1{\cdot}914 \pm 0{\cdot}249$; $R^2 = 0{\cdot}97$; $P < 0{\cdot}001$; Table S4). Furthermore, the scaling of growth for *Q. velutina* (dendrometer estimates only) and *F. grandifolia* (core estimates only; Table S5) was significantly less steep than stand-level scaling and consistent with the original MSTF prediction.

ENVIRONMENTAL VARIATION

In several cases, scaling was influenced by environmental conditions. First, the scaling of 2013 peak sap flux density in *F. grandifolia* was dependent on weather conditions (Fig. 5a). Similar to the stand-level relationship (Fig. 1f, Table S4), peak sap flux density was independent of tree size (as $z = 0{\cdot}016 \pm 0{\cdot}246$; $n = 7$, $P = 0{\cdot}9$, $R^2 = 0{\cdot}003$) on days with high evaporative demand (solar radiation >21·6 MJ m^{-2} day^{-1}, relative humidity <80%, wind speed >0·8 m s^{-1}). In contrast, on days with low evaporative demand (solar radiation <8·64 MJ m^{-2} day^{-1}, relative humidity >85%, wind speed <0·8 m s^{-1}), peak sap flux density increased with diameter ($z = 1{\cdot}058 \pm 0{\cdot}481$; $n = 7$, $P = 0{\cdot}007$, $R^2 = 0{\cdot}79$). Secondly, scaling of diameter growth differed between a drought year (1986; PDSI = −3·356) and a normal year (1985; PDSI = −0·866) for both stand- and species-level scaling (Fig. 4c; Table S5). Specifically, the ratio of drought year to normal year growth increased with DBH for all species combined

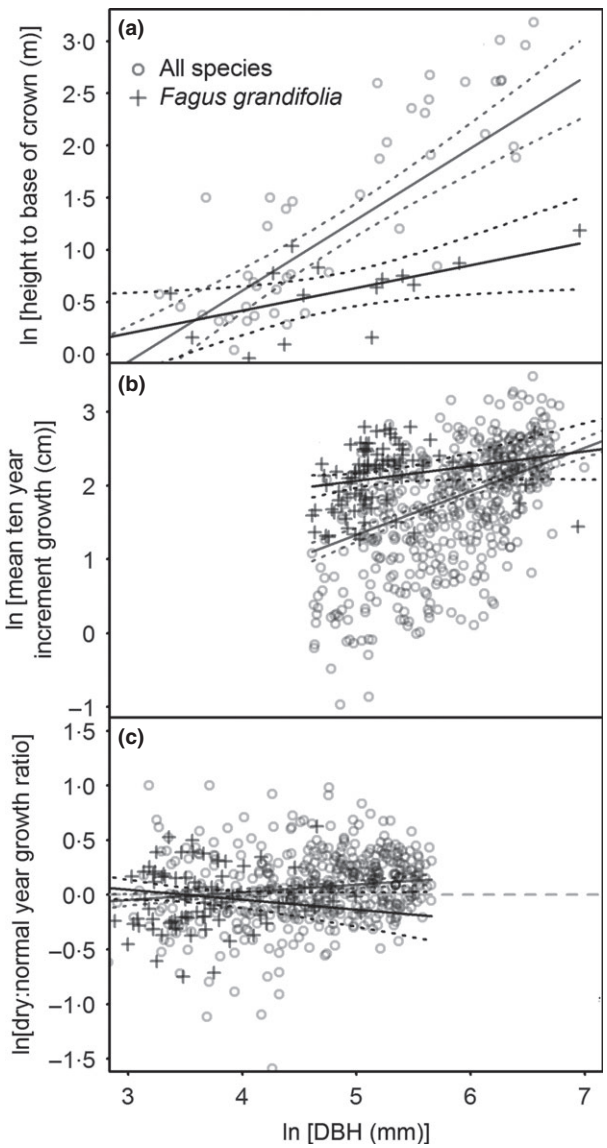

Fig. 4. Scaling relationships for *Fagus grandifolia* compared to other species for three variables: (a) height to base of crown, (b) increment growth (measured from cores) and (c) increment growth ratio in dry to normal year.

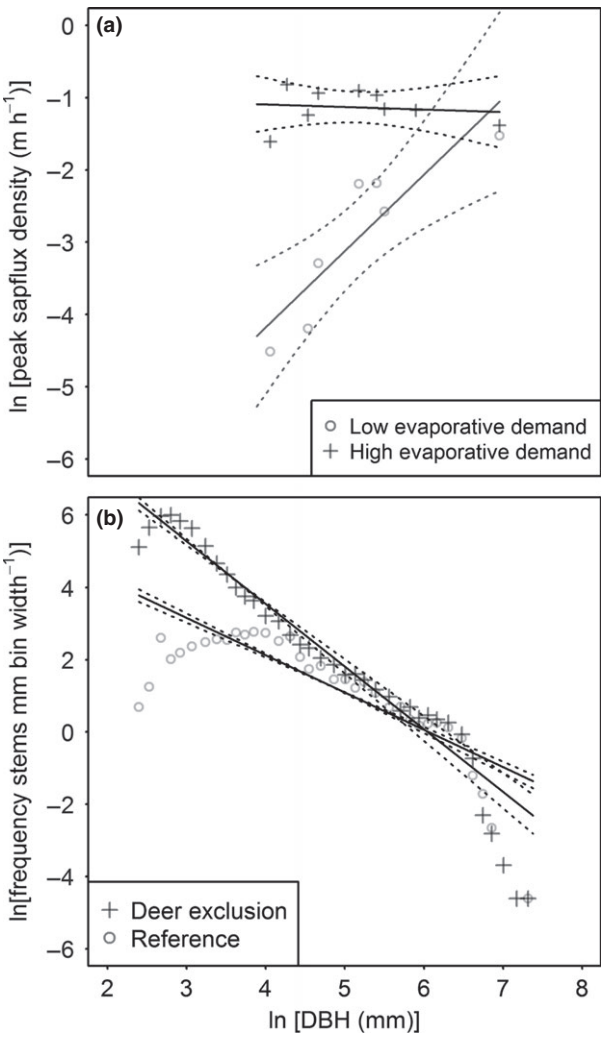

Fig. 5. Examples of variation in scaling relationships with environmental conditions: (a) scaling of daily peak sap flux density for *Fagus grandifolia* under conditions of high evaporative demand (solar radiation >21 6 MJ m^{-2} day^{-1}, relative humidity <80%, wind speed >0·8 m s^{-1}) and low evaporative demand (solar radiation <8·64 MJ m^{-2} day^{-1}, relative humidity >85%, wind speed <0·8 m s^{-1}) during the 2013 growing season; (b) Scaling of stem abundance (all species) inside and outside (in a reference plot; McGarvey *et al.* 2013) of deer exclosure.

($z = 0{\cdot}049 \pm 0{\cdot}033$; $P < 0{\cdot}001$) and for *Quercus spp.* ($z = 0{\cdot}067 \pm 0{\cdot}097$; $P = 0{\cdot}009$), while tending to decrease with DBH for *F. grandifolia* ($z = -0{\cdot}091 \pm 0{\cdot}104$; $P = 0{\cdot}08$). Finally, the scaling of stem abundance was strongly influenced by herbivory rates; stem abundance scaling exponents were $z = -1{\cdot}74$ (95% CI: $-1{\cdot}86$ to $-1{\cdot}56$; $R^2 = 0{\cdot}93$) for the deer exclusion area and $z = -1{\cdot}03$ (95% CI: $-1{\cdot}11$ to $-0{\cdot}96$; $R^2 = 0{\cdot}86$) for a reference plot (Table S7). This was driven by far greater abundance of small trees in the deer exclusion plot than in unprotected reference plot (Fig. 5b).

Discussion

Our findings show that existing scaling theory has mixed success at characterizing the scaling of structural, physiological and ecological traits of trees, with more recent models that predict a range of scaling exponents generally performing better than original MSTF predictions giving universal values for z (Table 1; Figs 1 and 2). Species-level scaling was variable, differing from stand-level scaling in roughly half the cases examined and reflecting ecological differences among species (Table 2, Figs 2 and 4). We also show evidence that scaling relationships can be strongly influenced by environmental variables including weather conditions and herbivore browsing pressure (Figs 4 and 5).

ASSESSMENT OF THEORETICAL PREDICTIONS

The original MSTF model describes how tree dimensions would scale for trees optimized for biomechanical stability and collection of homogeneously distributed resources (West, Brown & Enquist 1999b; Price *et al.* 2012). The scaling of tree height never deviated very substantially from the prediction that $z_h = 0{\cdot}67$ based on mechanical stability (prediction 1a, Table 1; Figs 1 and 2); however, significantly less steep scaling has been observed in Panama (Muller-Landau *et al.* 2006a) and pantropical data indicate that height scaling decelerates at larger diameters such that a power function overpredicts the height of the largest trees (Poorter, Bongers & Bongers 2006; Banin *et al.* 2012). A tendency for scaling to be less steep than projected for large trees could be driven by a variety of mechanisms affecting large trees that are not incorporated in the original MSTF prediction, including a shift in carbon allocation from height growth to sapwood or reproduction (Becker, Meinzer & Wullschleger 2000), hydraulic limitations (Ryan & Yoder 1997; Koch *et al.* 2004), and increased exposure to wind disturbance. Original MSTF predictions for scaling of crown dimensions (predictions 2a, 3a) are based upon assumptions of a homogeneous light environment and symmetrical self-similar branching that are not realistic and in particular deviates from reality in closed-canopy forests where competition for light strongly influences the scaling of crown dimensions (Mäkelä & Valentine 2006; Coomes *et al.* 2012). A modified model that relaxes these assumptions leads to a range of potential scaling exponents (Smith *et al.* 2014), as was observed here (Fig. 2). As the scaling of tree dimensions affects predictions of the scaling of hydraulics and ecology (Sperry *et al.* 2012; Smith *et al.* 2014), it should not be expected that stands deviating substantially from original MSTF predictions for tree dimensions would conform to those for water use and growth.

The original MSTF model did not depict a fully realistic optimization of plant hydraulics (Mencuccini 2002; Sperry, Meinzer & McCulloh 2008; Price *et al.* 2012; Sperry *et al.* 2012). One simplifying assumption was constant sapwood area to basal area ratio such that sapwood area scales with $z_{As} = 2$ – an approximation that is only sometimes realistic (Figs 1–3; Tables 1-2). More realistic approximations of the scaling of sapwood area – that is, $1 \leq z_{As} \leq 2$ (Figs 2 and 3; Table S3) – have since been incorporated into a modified model (prediction 4b, Table 1; Sperry *et al.* 2012). Another assumption of the original MSTF model was that peak sap flux density is independent of DBH (5a; Table 1). While this assumption was supported for seasonally averaged, stand-level data at SCBI (Fig. 1f), it is not universally true (Figs 2 and 5a; Table S8; Schäfer, Oren & Tenhunen 2000; Meinzer, Goldstein & Andrade 2001). Drawing upon the assumption about the scaling of sapwood area and peak sap flux density, the original MSTF prediction is that transpiration will scale as the product of sapwood area ($z_{As} = 2$) and sap flux density ($z_{Fd,max} = 0$), or in direct proportion to the number of leaves, with a scaling exponent of $z_{Fmax} = 2$ (prediction 6a; Table 2; West, Brown & Enquist 1999b). At SCBI, the significantly less steep scaling of peak transpiration relative to this prediction is in part a logical consequence of the fact that the zs for crown area, crown volume and sapwood area were all lower than expected based on the original MSTF model (Fig. 1). It is also driven by the fact that our calculations account for the fact that sap flux density varies by radial depth in the stem (Gebauer, Horna & Leuschner 2008), which are not incorporated in the original MSTF model. Further, the original MSTF model does not account for a variety of factors known to influence the scaling of peak transpiration rates, including the effects of gravity, hydraulic resistance, the ratio of sapwood area to basal area. A recent modification to the original MSTF model, which incorporated a number of these factors, yielded a range of potential scaling exponents (prediction 6b, Table 1; Sperry *et al.* 2012), and observations at SCBI fell within this range. Still, there remain some mechanisms not currently incorporated into theoretical predictions that may have an important influence on the scaling of transpiration. Of particular importance for scaling in forests, both the original MSTF model and modifications thereof (Table 1) assume an equal soil-to-canopy pressure gradient across tree size classes – an assumption that is commonly violated in closed-canopy forests, where atmospheric moisture demand tends to be higher for canopy than for understorey positions (e.g. Roberts, Cabral & Aguiar 1990).

Given that transpiration and photosynthesis are closely coupled, accurate prediction of the scaling of transpiration is critical to predicting the scaling of tree growth.

The original MSTF prediction for the scaling of diameter growth (7a; Table 1), which is derived based on the assumptions that whole-tree photosynthesis scales with the same exponent as transpiration and that all tree size classes experience similar environments, failed to accurately characterize the scaling of diameter growth at SCBI or other forests globally (Figs 1 and 2). The underlying assumption that all trees experience equal environmental conditions is clearly violated in a forest, where asymmetric competition for light results in steeper growth scaling (prediction 7b, Table 1; Muller-Landau *et al.* 2006a; Coomes & Allen 2009; Coomes, Lines & Allen 2011; Rüger & Condit 2012). The present study adds to our understanding of the mechanisms underlying diameter growth scaling by showing that the scaling of peak transpiration is not steeper than predicted by the original MSTF model (Figs 1 and 2). Rather, there are several assumptions linking peak transpiration to diameter growth that may be unrealistic for a closed-canopy forest. Specifically, theory currently fails to account for the following: (i) annual transpiration may not scale with the same exponent as peak transpiration because daily patterns in sap flux density, leaf phenology and responses to variable environmental conditions all vary with tree size (Fig. 5a; Meinzer, Goldstein & Andrade 2001; Augspurger & Bartlett 2003); (ii) water use efficiency – i.e., the ratio of C assimilated in photosynthesis to transpiration – varies with tree size, in part because tall trees receive more light (McDowell *et al.* 2011); (iii) there may be size-related differences in carbon use efficiency, allocation to woody growth as opposed to leaves, roots or reproduction, and systematic differences in wood density with tree age or canopy position (Naidu, DeLucia & Thomas 1998; Becker, Meinzer & Wullschleger 2000). Moreover, diameter growth rate may be reduced in closed-canopy forests where self-pruning in response to low light conditions reduces crown volume relative to what it might be in the absence of light competition (Coomes *et al.* 2012). There remains a lot of variation in diameter growth rates that cannot be accounted for by existing theory; a power function failed to account for substantial nonlinearity in growth scaling for the smallest trees at SCBI and explained relatively little variation when data were not binned by size class (Fig. 1). Further development of theory will be necessary to derive specific mechanistic predictions for the scaling of tree growth rate in closed-canopy forests.

The original MSTF prediction for the scaling of mortality rate (prediction 8a; Table 1) is based on a broad tendency for mortality rate to be inversely correlated with mass-specific growth rate (Brown *et al.* 2004). Given that observed growth scaling exponents are almost always higher than originally predicted by MSTF (Fig. 2; Table 1), the fact that empirically observed mortality scaling exponents tended to be higher than the original MSTF prediction (Fig. 2) is roughly consistent with the expectation that mortality rate scales as the inverse of mass-specific biomass growth rate. However, the corresponding prediction that $z_M = z_{\mathrm{Gd}} - 1$ (8b; Table 1) was quantitatively supported for only 3 of 14 stand-level relationships examined here (including SCBI; Table 1), indicating that an inverse correlation between mortality rate and mass-specific growth rate is insufficient to fully explain the scaling of mortality rate. This is unsurprising, given that MSTF predictions (8a and 8b; Table 1) do not account for a number of mechanisms, including the commonly observed increase in mortality in the largest-diameter trees resulting in a 'U-shaped' mortality pattern, which is particularly pronounced in old-growth forests (prediction 8c; Table 1; Coomes *et al.* 2003; Coomes & Allen 2007). While such an increase occurs at SCBI (Fig. 1k), it may be less pronounced than in other forests given the fact that SCBI is not old-growth forest.

Stem abundance distributions are shaped 'bottom-up' by the scaling of growth and mortality (e.g., Muller-Landau *et al.* 2006b) and 'top-down' by partitioning of resources across size classes (e.g., West, Enquist & Brown 2009). Although growth and mortality do not scale according to original MSTF predictions, conformation of size distributions to the original MSTF prediction (9a, Table 1) might be expected if top-down mechanisms dominate. At the stand level, the SCBI forest had a lower z_N and fewer small (DBH <2·5 cm) and very large (DBH > 80 cm) individuals than expected based on the original MSTF prediction of a power function distribution with $z_N = -2$ (Fig. 1l). Stem abundance may be reduced in small size classes by deer browsing (Fig. 5c; McGarvey *et al.* 2013) and in large size classes by historical deforestation (Bourg *et al.* 2013). As at SCBI, tree size distributions deviate from a power function with $z_N = -2$ in most forests world-wide, being influenced by stand age, disturbance and environmental factors such as aridity and wind exposure (Fig. 2a; Enquist & Niklas 2001; Muller-Landau *et al.* 2006b; Coomes & Allen 2007; Enquist, West & Brown 2009; Hale *et al.* 2012). These deviations point to incomplete representation of the factors shaping tree size distributions. Better understanding of these mechanisms in forests globally holds promise for understanding forest structure and could prove useful as a rapid means for estimating biomass based on the abundance of the largest trees (e.g. Slik *et al.* 2013).

SPECIES-LEVEL SCALING

Species-level scaling parameters varied among species and often deviated from stand-level scaling patterns (Table 2; Figs 2–4). This variation reflects a diversity of ecological strategies, which is the basis for competitive advantage (Davies 2001; Pretzsch & Dieler 2012). At SCBI, for instance, the hydrophilic, shade-tolerant *Fagus grandifolia* has deeper crowns than other trees of its size (Fig. 4a), thicker sapwood (Fig. 3), a tendency towards higher sap flux density and total transpiration (Table S4), less steep

growth-diameter scaling (Figs 2 and 4b), and a greater drought sensitivity of large trees compared with small ones than was not observed in other species (Fig. 4c). In contrast, the light-demanding, early successional *Liriodendron tulipifera* had steeper scaling of sapwood area, sap flux density, transpiration, diameter growth and mortality relative to other species (Tables S3-S6), which helps to explain the tendency for this species to thrive as a canopy dominant but not in the understorey. The low abundance of small *L. tulipifera* trees was reflected in its less steep scaling of stem abundance. The diversity of scaling strategies across species implies that, while theory can provide useful first-order predictions, more nuanced models are required to capture the range of possible scaling exponents (Sperry, Meinzer & McCulloh 2008; Sperry *et al.* 2012; Smith *et al.* 2014). It also implies that stand-level scaling patterns are shaped by species composition.

We also observed evidence of how perturbations can underlie anomalous species-level scaling relationships. *Ulmus rubra* suffered recent decline at SCBI, with 52% mortality between 2008 and 2013. The probable cause was Dutch elm disease; *Ulmus americana* concurrently suffered 36% mortality rate, and a field survey identified bark beetle galleries on ~80% of trees visited (Gonzalez-Akre & McGarvey, unpublished data). Larger trees were more strongly affected; mortality increased with tree size, contrasting with the typical pattern of negative mortality rate scaling (Fig. 2). This example provides evidence that species-level scaling relationships should not be viewed as static, but as influenced by variable environmental conditions.

ENVIRONMENTAL VARIATION

Size-related scaling of physiological and ecological characteristics can vary with environmental conditions. Two of the instances documented here – variation in the scaling of sap flux density with weather conditions (Fig. 5a) and a declining ratio of growth in a drought year to that of a regular year (Fig. 4c; *Fagus grandifolia*) – illustrate how trees of different sizes respond differently to climatic variation. Because scaling relationships vary with climate variables through space and time, climate change is likely to have differential effects on trees of different sizes, with potentially significant consequences at the ecosystem level. Scaling relationships are also influenced by browsing; twenty years of deer exclusion at this site has strikingly increased the abundance of small trees and therefore steepened the scaling of stem abundance (Fig. 5b; McGarvey *et al.* 2013). Currently, theory does little to address the role of environmental conditions on scaling relationships. Understanding the interaction of scaling parameters with environmental conditions (e.g. Lines *et al.* 2012) may provide critical insights into forest responses to global change.

Together, the observed variations in scaling relationships across species and environmental conditions indicate that stand-level, time-averaged scaling relationships – for example, stand-level scaling of diameter growth over five or ten years (Fig. 1h,j) – are underlain by a complex diversity of species-level scaling relationships that can vary substantially with fluctuating environmental conditions (e.g. Figs 4c and 5a). Importantly, while instantaneous species-level scaling relationships determine stand-level and time-averaged scaling relationships, stand-level performance will often differ from the mean scaling derived via averages across species or across time (Fig. 2; Ruel & Ayres 1999). Thus, stand-level scaling laws should be universal, *sensu* original MSTF predictions, only to the extent that they characterize emergent responses of forest communities to physical and biological forces that tightly constrain inhabitable niche space and are invariant in space and time. In contrast, if species-level scaling and community composition are not strongly shaped by stand-level constraints on scaling, or to the extent that the environmental conditions that shape stand-level scaling vary in time and space, we should not expect to observe 'universal' scaling in forests.

Conclusions

We have demonstrated that existing scaling theory has mixed success at describing scaling relationships in closed-canopy forests (Figs 1 and 2) and that there is rich variety in scaling relationships associated with species differences and environmental variation (Figs 2–5). While theory has generated first-order predictions that can provide decent approximations on a macroecological scale (Table 1; Figs 1 and 2), a more nuanced mechanistic understanding of scaling relationships is necessary to accurately characterize forest dynamics and predict responses to global change (Coomes 2006). Specifically, it would be valuable to expand theory to describe (i) how scaling parameters are influenced by differences in the average abiotic environment experienced by trees of different sizes, (ii) how scaling relationships interact with functional traits to produce a diversity of species-level scaling patterns and (iii) how spatially and temporally variable environmental conditions influence scaling parameters. Such a mechanistic understanding will be particularly valuable in the current era of global change, when improved understanding of forest ecosystems and their interactions with the climate system is critical to climate change prediction and mitigation.

Acknowledgements

We thank all interns and volunteers who have helped with fieldwork at SCBI; Evan DeLucia, Mike Masters, Alex Bohleber, Tara Hudiburg and Matteo Detto for help with sap flow system construction; and Elizabeth Dougan and Suzanne Sine for help with purchasing; and Adam Miller, David Coomes, and an anonymous reviewer for helpful feedback. This research was funded by a Smithsonian CGPS grant to KJAT, SMM and G. G. Parker.

Data accessibility

Data from the initial (2008) census of the SCBI CTFS-ForestGEO site and radial growth increments derived from tree cores have been published

(Bourg *et al.* 2013; DOI: 10.1890/13-0010.1). Additional data from the SCBI CTFS-ForestGEO site underlying all analyses reported here are accessible at the Dryad Digital Repository: doi: doi:10.5061/dryad.6nc8c; Anderson-Teixeira *et al.* 2015b). Scaling exponents from forests world-wide (Fig. 2a) are given in the Appendix (Table S8).

References

Anderson-Teixeira, K.J., Miller, A.D., Mohan, J.E., Hudiburg, T.W., Duval, B.D. & DeLucia, E.H. (2013) Altered dynamics of forest recovery under a changing climate. *Global Change Biology*, **19**, 2001–2021.

Anderson-Teixeira, K.J., Davies, S.J., Bennett, A.C., Gonzalez-Akre, E.B., Muller-Landau, H.C., Joseph Wright, S. *et al.* (2015a) CTFS-ForestGEO: a worldwide network monitoring forests in an era of global change. *Global Change Biology*, **21**, 528–549.

Anderson-Teixeira, K.J., McGarvey, J.C., Muller-Landau, H.C., Park, J.Y., Gonzalez-Akre, E.B., Herrmann, V. *et al.* (2015b) Data from: Size-related scaling of tree form and function in a mixed-age forest. Dryad Digital Repository http://doi:10.5061/dryad.6nc8c

Anfodillo, T., Carrer, M., Simini, F., Popa, I., Banavar, J.R. & Maritan, A. (2013) An allometry-based approach for understanding forest structure, predicting tree-size distribution and assessing the degree of disturbance. *Proceedings of the Royal Society B: Biological Sciences*, **280**, 20122375.

Augspurger, C.K. & Bartlett, E.A. (2003) Differences in leaf phenology between juvenile and adult trees in a temperate deciduous forest. *Tree Physiology*, **23**, 517–525.

Banin, L., Feldpausch, T.R., Phillips, O.L., Baker, T.R., Lloyd, J., Affum-Baffoe, K. *et al.* (2012) What controls tropical forest architecture? Testing environmental, structural and floristic drivers. *Global Ecology and Biogeography*, **21**, 1179–1190.

Becker, P., Meinzer, F.C. & Wullschleger, S.D. (2000) Hydraulic limitation of tree height: a critique. *Functional Ecology*, **14**, 4–11.

Bourg, N.A., McShea, W.J., Thompson, J.R., McGarvey, J.C. & Shen, X. (2013) Initial census, woody seedling, seed rain, and stand structure data for the SCBI SIGEO Large Forest Dynamics Plot: *Ecological Archives* E094-195. *Ecology*, **94**, 2111–2112.

Brown, J.H., Gillooly, J.F., Allen, A.P., Savage, V.M. & West, G.B. (2004) Toward a metabolic theory of ecology. *Ecology*, **85**, 1771–1789.

Condit, R.S. (1998) *Tropical Forest Census Plots - Methods and Results From Barro Colorado Island, Panama and a Comparison With Other Plots*. Springer-Verlag, Berlin, and R. G. Landes Company, Georgetown, Texas, USA.

Coomes, D.A. (2006) Challenges to the generality of WBE theory. *Trends in Ecology & Evolution*, **21**, 593–596.

Coomes, D.A. & Allen, R.B. (2007) Mortality and tree-size distributions in natural mixed-age forests. *Journal of Ecology*, **95**, 27–40.

Coomes, D.A. & Allen, R.B. (2009) Testing the Metabolic Scaling Theory of tree growth. *Journal of Ecology*, **97**, 1369–1373.

Coomes, D.A., Lines, E.R. & Allen, R.B. (2011) Moving on from Metabolic Scaling Theory: hierarchical models of tree growth and asymmetric competition for light. *Journal of Ecology*, **99**, 748–756.

Coomes, D., Duncan, R., Allen, R. & Truscott, J. (2003) Disturbances prevent stem size-density distributions in natural forests from following scaling relationships. *Ecology Letters*, **6**, 980–989.

Coomes, D.A., Holdaway, R.J., Kobe, R.K., Lines, E.R. & Allen, R.B. (2012) A general integrative framework for modelling woody biomass production and carbon sequestration rates in forests. *Journal of Ecology*, **100**, 42–64.

Davies, S.J. (2001) Tree mortality and growth in 11 sympatric macaranga species in Borneo. *Ecology*, **82**, 920–932.

Enquist, B. & Niklas, K. (2001) Invariant scaling relations across tree-dominated communities. *Nature*, **410**, 655–660.

Enquist, B.J., West, G.B. & Brown, J.H. (2009) Extensions and evaluations of a general quantitative theory of forest structure and dynamics. *Proceedings of the National Academy of Sciences of the United States of America*, **106**, 7046–7051.

Gebauer, T., Horna, V. & Leuschner, C. (2008) Variability in radial sap flux density patterns and sapwood area among seven co-occurring temperate broad-leaved tree species. *Tree Physiology*, **28**, 1821–1830.

Granier, A. (1985) A new method of sap flow measurement in tree stems. *Annales Des Sciences Forestieres*, **42**, 193–200.

Hale, S.E., Gardiner, B.A., Wellpott, A., Nicoll, B.C. & Achim, A. (2012) Wind loading of trees: influence of tree size and competition. *European Journal of Forest Research*, **131**, 203–217.

Koch, G.W., Sillett, S.C., Jennings, G.M. & Davis, S.D. (2004) The limits to tree height. *Nature*, **428**, 851–854.

Lai, J., Coomes, D.A., Du, X., Hsieh, C., Sun, I.-F., Chao, W.-C. *et al.* (2013) A general combined model to describe tree-diameter distributions within subtropical and temperate forest communities. *Oikos*, **122**, 1636–1642.

Lines, E.R., Zavala, M.A., Purves, D.W. & Coomes, D.A. (2012) Predictable changes in aboveground allometry of trees along gradients of temperature, aridity and competition. *Global Ecology and Biogeography*, **21**, 1017–1028.

Mäkelä, A. & Valentine, H.T. (2006) Crown ratio influences allometric scaling in trees. *Ecology*, **87**, 2967–2972.

Malhi, Y., Phillips, O.l., Lloyd, J., Baker, T., Wright, J., Almeida, S. *et al.* (2002) An international network to monitor the structure, composition and dynamics of Amazonian forests (RAINFOR). *Journal of Vegetation Science*, **13**, 439–450.

Mascaro, J., Asner, G.P., Muller-Landau, H.C., van Breugel, M., Hall, J. & Dahlin, K. (2011) Controls over aboveground forest carbon density on Barro Colorado Island, Panama. *Biogeosciences*, **8**, 1615–1629.

McDowell, N.G., Bond, B.J., Hill, L., Ryan, M.G. & Whitehead, D. (2011) Relationship between tree height and carbon isotope discrimination. *Size and age Related Changes in Tree Structure and Function* (eds F.C. Meinzer & U. Niinemets), pp. 255–286. Springer Publishing, Dordrecht.

McGarvey, J.C., Bourg, N.A., Thompson, J.R., McShea, W.J. & Shen, X. (2013) Effects of twenty years of deer exclusion on woody vegetation at three life-history stages in a mid-atlantic temperate deciduous forest. *Northeastern Naturalist*, **20**, 451–468.

McMahon, T.A. & Kronauer, R.E. (1976) Tree structures: Deducing the principle of mechanical design. *Journal of Theoretical Biology*, **59**, 443–466.

Meinzer, F.C., Goldstein, G. & Andrade, J.L. (2001) Regulation of water flux through tropical forest canopy trees: do universal rules apply? *Tree Physiology*, **21**, 19–26.

Meinzer, F.C., Andrade, J.L., Goldstein, G., Holbrook, N.M., Cavelier, J. & Wright, S.J. (1999) Partitioning of soil water among canopy trees in a seasonally dry tropical forest. *Oecologia*, **121**, 293–301.

Meinzer, F.C., James, S.A., Goldstein, G. & Woodruff, D. (2003) Whole-tree water transport scales with sapwood capacitance in tropical forest canopy trees. *Plant, Cell & Environment*, **26**, 1147–1155.

Mencuccini, M. (2002) Hydraulic constraints in the functional scaling of trees. *Tree Physiology*, **22**, 553–565.

Moorcroft, P.R., Hurtt, G.C. & Pacala, S.W. (2001) A method for scaling vegetation dynamics: the ecosystem demography model (ED). *Ecological Monographs*, **71**, 557–586.

Muller-Landau, H.C., Condit, R.S., Chave, J., Thomas, S.C., Bohlman, S.A., Bunyavejchewin, S. *et al.* (2006a) Testing metabolic ecology theory for allometric scaling of tree size, growth and mortality in tropical forests. *Ecology Letters*, **9**, 575–588.

Muller-Landau, H.C., Condit, R.S., Harms, K.E., Marks, C.O., Thomas, S.C., Bunyavejchewin, S. *et al.* (2006b) Comparing tropical forest tree size distributions with the predictions of metabolic ecology and equilibrium models. *Ecology Letters*, **9**, 589–602.

Naidu, S.L., DeLucia, E.H. & Thomas, R.B. (1998) Contrasting patterns of biomass allocation in dominant and suppressed loblolly pine. *Canadian Journal of Forest Research*, **28**, 1116–1124.

National Climatic Data Center (2013) *Time Bias Corrected Divisional Temperature-Precipitation-Drought Index*. National Climatic Data Center, Asheville.

Niklas, K.J. (1994) *Plant Allometry: The Scaling of Form and Process*. University of Chicago Press, Chicago, Illinois, USA.

Niklas, K.J. & Spatz, H.-C. (2004) Growth and hydraulic (not mechanical) constraints govern the scaling of tree height and mass. *Proceedings of the National Academy of Sciences of the United States of America*, **101**, 15661–15663.

Phillips, O.L., van der Heijden, G., Lewis, S.L., López-González, G., Aragão, L.E.O.C., Lloyd, J. *et al.* (2010) Drought–mortality relationships for tropical forests. *New Phytologist*, **187**, 631–646.

Poorter, L., Bongers, L. & Bongers, F. (2006) Architecture of 54 moist-forest tree species: traits, trade-offs, and functional groups. *Ecology*, **87**, 1289–1301.

Poorter, L., Wright, S.J., Paz, H., Ackerly, D.D., Condit, R., Ibarra-Manríquez, G. *et al.* (2008) Are functional traits good predictors of demographic rates? Evidence from five neotropical forests. *Ecology*, **89**, 1908–1920.

Pretzsch, H. & Dieler, J. (2012) Evidence of variant intra- and interspecific scaling of tree crown structure and relevance for allometric theory. *Oecologia*, **169**, 637–649.
Price, C.A., Ogle, K., White, E.P. & Weitz, J.S. (2009) Evaluating scaling models in biology using hierarchical Bayesian approaches. *Ecology Letters*, **12**, 641–651.
Price, C.A., Weitz, J.S., Savage, V.M., Stegen, J., Clarke, A., Coomes, D.A. *et al.* (2012) Testing the metabolic theory of ecology. *Ecology Letters*, **15**, 1465–1474.
Purves, D. & Pacala, S. (2008) Predictive models of forest dynamics. *Science*, **320**, 1452–1453.
Roberts, J., Cabral, O.M.R. & Aguiar, L.F.D. (1990) Stomatal and boundary-layer conductances in an amazonian terra firme rain forest. *Journal of Applied Ecology*, **27**, 336–353.
Ruel, J.J. & Ayres, M.P. (1999) Jensen's inequality predicts effects of environmental variation. *Trends in Ecology & Evolution*, **14**, 361–366.
Rüger, N. & Condit, R. (2012) Testing metabolic theory with models of tree growth that include light competition. *Functional Ecology*, **26**, 759–765.
Ryan, M.G. & Yoder, B.J. (1997) Hydraulic limits to tree height and tree growth. *BioScience*, **47**, 235–242.
Savage, V.M., Bentley, L.P., Enquist, B.J., Sperry, J.S., Smith, D.D., Reich, P.B. *et al.* (2010) Hydraulic trade-offs and space filling enable better predictions of vascular structure and function in plants. *Proceedings of the National Academy of Sciences of the United States of America*, **107**, 22722–22727.
Schäfer, K.V.R., Oren, R. & Tenhunen, J.D. (2000) The effect of tree height on crown level stomatal conductance. *Plant, Cell & Environment*, **23**, 365–375.
Sibly, R.M., Brown, J.H. & Kodric-Brown, A. (eds) (2012) *Metabolic Ecology: A Scaling Approach.* Wiley-Blackwell, Chichester, West Sussex, Hoboken, New Jersey, USA.
Simini, F., Anfodillo, T., Carrer, M., Banavar, J.R. & Maritan, A. (2010) Self-similarity and scaling in forest communities. *Proceedings of the National Academy of Sciences of the United States of America*, **107**, 7658–7662.
Slik, J.W.F., Paoli, G., McGuire, K., Amaral, I., Barroso, J., Bastian, M. *et al.* (2013) Large trees drive forest aboveground biomass variation in moist lowland forests across the tropics: large trees and tropical forest biomass. *Global Ecology and Biogeography*, **22**, 1261–1271.
Smith, D.D., Sperry, J.S., Enquist, B.J., Savage, V.M., McCulloh, K.A. & Bentley, L.P. (2014) Deviation from symmetrically self-similar branching in trees predicts altered hydraulics, mechanics, light interception and metabolic scaling. *New Phytologist*, **201**, 217–229.
Sperry, J.S., Meinzer, F.C. & McCulloh, K.A. (2008) Safety and efficiency conflicts in hydraulic architecture: scaling from tissues to trees. *Plant, Cell & Environment*, **31**, 632–645.
Sperry, J.S., Smith, D.D., Savage, V.M., Enquist, B.J., McCulloh, K.A., Reich, P.B. *et al.* (2012) A species-level model for metabolic scaling in trees I. Exploring boundaries to scaling space within and across species. *Functional Ecology*, **26**, 1054–1065.
Vertessy, R.A., Benyon, R.G., O'Sullivan, S.K. & Gribben, P.R. (1995) Relationships between stem diameter, sapwood area, leaf area and transpiration in a young mountain ash forest. *Tree Physiology*, **15**, 559–567.
West, G., Brown, J. & Enquist, B. (1999a) The fourth dimension of life: fractal geometry and allometric scaling of organisms. *Science*, **284**, 1677–1679.
West, G.B., Brown, J.H. & Enquist, B.J. (1999b) A general model for the structure and allometry of plant vascular systems. *Nature*, **400**, 664–667.
West, G.B., Enquist, B.J. & Brown, J.H. (2009) A general quantitative theory of forest structure and dynamics. *Proceedings of the National Academy of Sciences of the United States of America*, **106**, 7040–7045.
White, E.P., Xiao, X., Nick, J.B. & Sibly, R.M. (2012) Methodological Tools. *Metabolic Ecology: A Scaling Approach* (eds R.M. Sibly, J.H. Brown & A. Kodric-Brown), pp. 9–20. Wiley-Blackwell, Chichester, West Sussex.
Woudenberg, S.W., Conkling, B.L., O'Connell, B.M., LaPoint, E.B., Turner, J.A. & Waddell, K.L. (2010) *The Forest Inventory and Analysis Database: Database description and users manual version 4.0 for Phase 2*. Gen. Tech. Rep. RMRS- GTR-245, 336 pp. U.S. Department of Agriculture, Forest Service, Rocky Mountain Research Station, Fort Collins, CO.
Wullschleger, S.D., Hanson, P. & Todd, D. (2001) Transpiration from a multi-species deciduous forest as estimated by xylem sap flow techniques. *Forest Ecology and Management*, **143**, 205–213.

Received 10 July 2014; accepted 28 April 2015
Handling Editor: Emma Sayer

Supporting Information

Additional Supporting information may be found in the online version of this article:

Appendix S1. Complete Methodology.
Table S1. Stem abundance and biomass of dominant canopy species at SCBI.
Table S2. Scaling relationships between DBH and tree dimensions.
Table S3. Scaling relationships between DBH and sapwood radius, bark thickness, and sapwood area.
Table S4. Scaling relationships between DBH and median growing season sap flow.
Table S5. Scaling relationships between DBH and diameter growth.
Table S6. Scaling relationships between DBH and mortality.
Table S7. Scaling relationships between DBH and stem abundance.
Table S8. Record of scaling exponents observed in closed-canopy forests worldwide